Electronic Supplementary Material (ESI) for CrystEngComm

$CaCO_3$ Nanostructured Crystals Induced by Nacreous Organic Extracts

Yao-Hung Tseng,[*a,b,†] Corinne Chevallard,[a] Yannicke Dauphin[b] and Patrick Guenoun[a]

S1. Structure of the shell of Pinctada margaritifera pearl oyster.

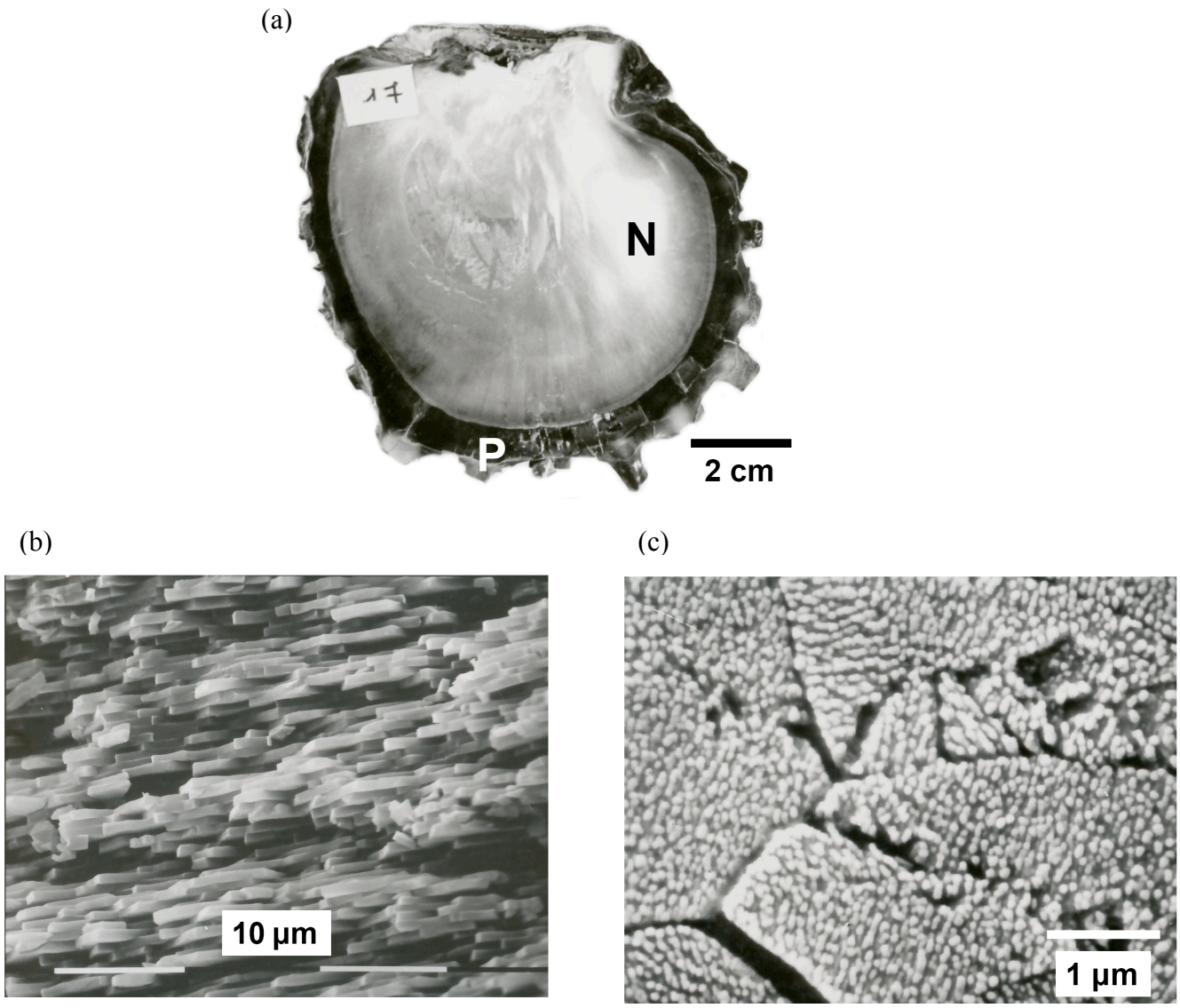

Figure S1. (a) Inner view of a valve of the shell of Pinctada margaritifera, showing the nacreous layer (N) and the outer prismatic calcitic layer (P). (b) SEM image of the brick and mortar patterns of the nacre in Pinctada margaritifera. (c) Inner structure of a nacreous tablet, showing aligned granules. The sample is fixed and etched by glutaraldehyde, acetic acid and alcian blue for 10 min before measurements.

S2. Analysis of SOM composition.

Although pearl oyster nacre is probably the best known shell layer among biogenic carbonates, the organic components are not yet deciphered. Extraction procedures differ, but usually a soluble and an insoluble organic fractions are separated. The classical hypothesis emphasizes the role of the soluble organic matrices (SOM) in the biomineralization mechanisms. Thus, the bulk properties are known (molecular weights, pI, amino acid composition, etc.). Nevertheless, due to the abundance and variety of components (proteins, sugars) of the SOM, only a few proteins have been isolated and identified, and their role is the biomineralization process is not well established.

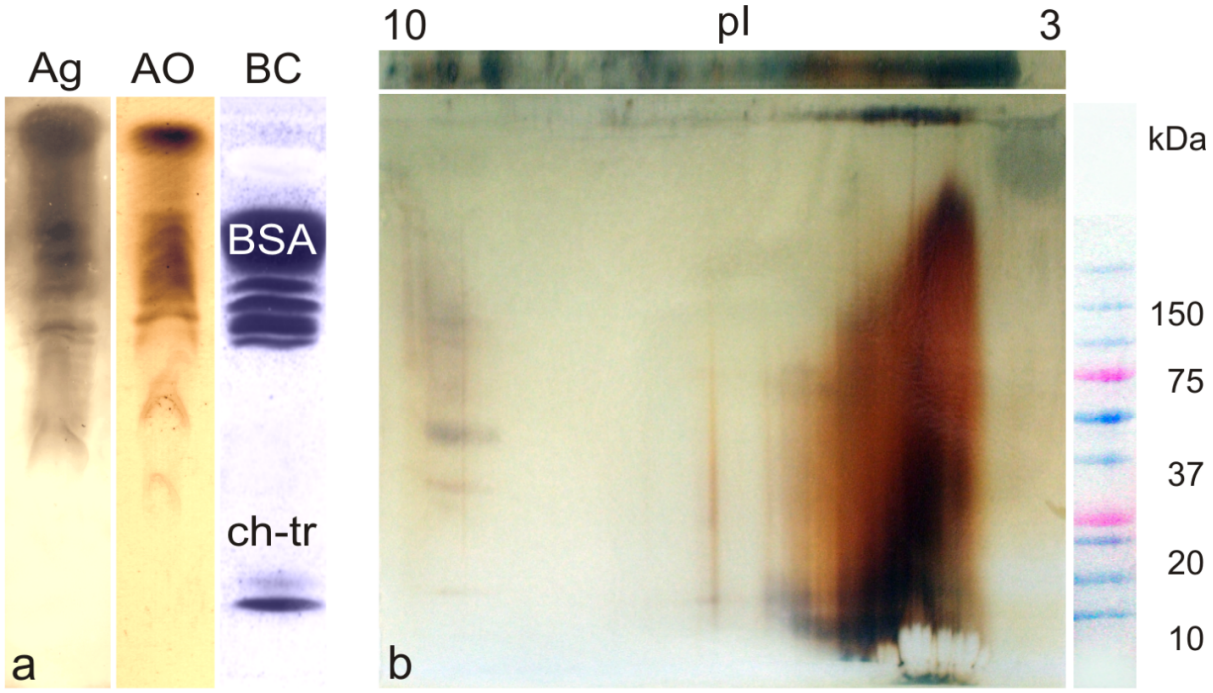

Figure S2. (a) Isoeletric focusing (IEF) of the SOM, stained using silver (Ag) for proteins and glycoproteins, and acridine orange (AO) for acidic sulfated sugars. Bovine serum albumin (BSA) (pI from 5.2 to 5.6) and chymotrypsin (ch-tr) (pI =9.1) were used as reference for pI stained using Coomassie blue (BC). (b) Two dimensional gel electrophoresis stained using Ag for proteins and glycoproteins. In both cases, acidic components are abundant. The IEF and staining procedures are described in Y. Dauphin, *J. Biol. Chem.*, 2003, 278 (17) , 15168-15177.

S3. UV-Vis spectrum of SOM solutions.

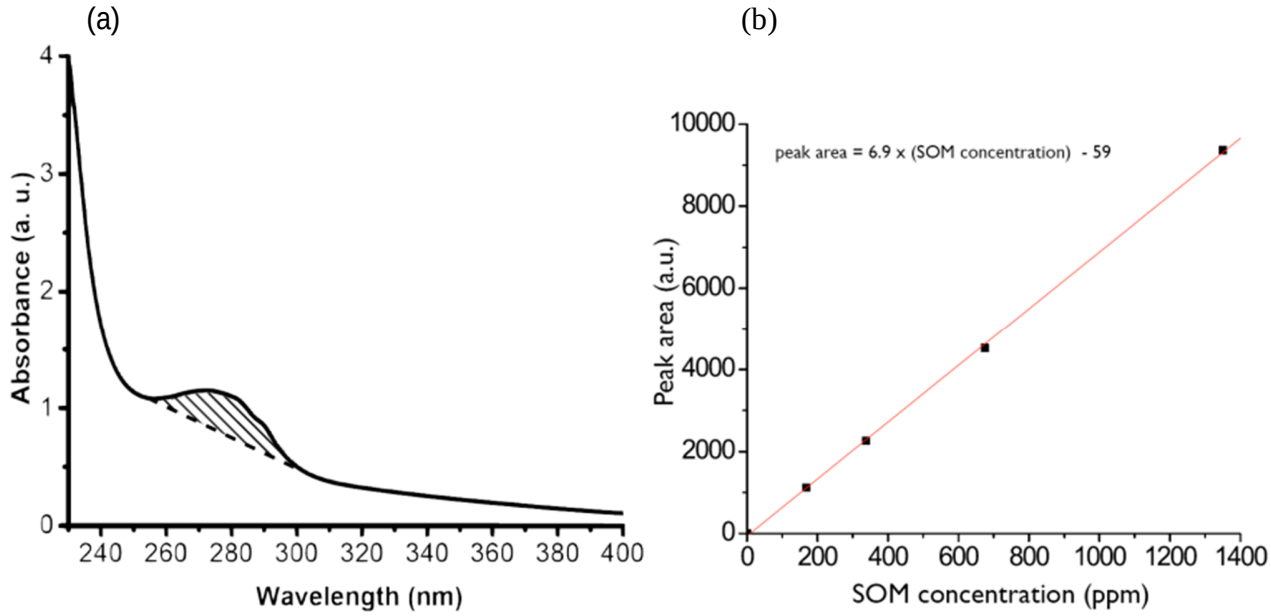

Figure S3 (a).UV-Vis spectrum of 1350 ppm SOM solution. The oblique region is used to calculate the integral of the pear area**.** (b).The calibration line is created by monitoring different integrals of peak area in a series of SOM concentrations.

S4. Influence of SOM concentration on final pH.

	SOM concentration (ppm)						
	0	3.1	6.3	12.5	25	50	100
pH	6.5	6.9	7.2	7.4	7.4	7.6	7.6

Table S4. pH values of the solution and the weight of the precipitates after reaction for 1 day with different concentrations of SOM; the starting amount of $CaCO_3$ is 2.5×10^{-4} moles for each solution with initial pH value of 7.7.

S5. SEM micrographs of $CaCO_3$-50ppm sample.

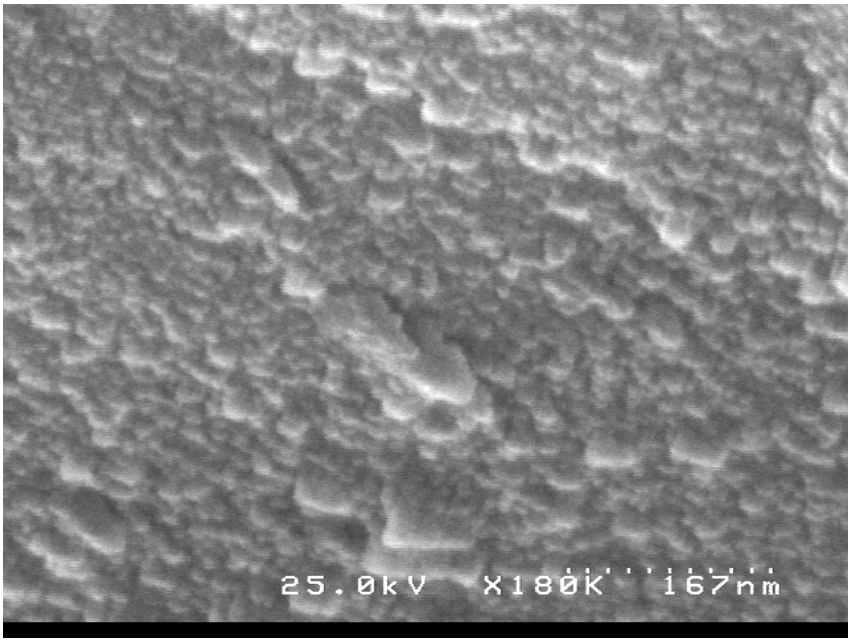

Figure S5. SEM image of $CaCO_3$-50ppm sample shows the layer is composed of nanoparticles.

S6. TGA profiles of $CaCO_3$ –SOM composites.

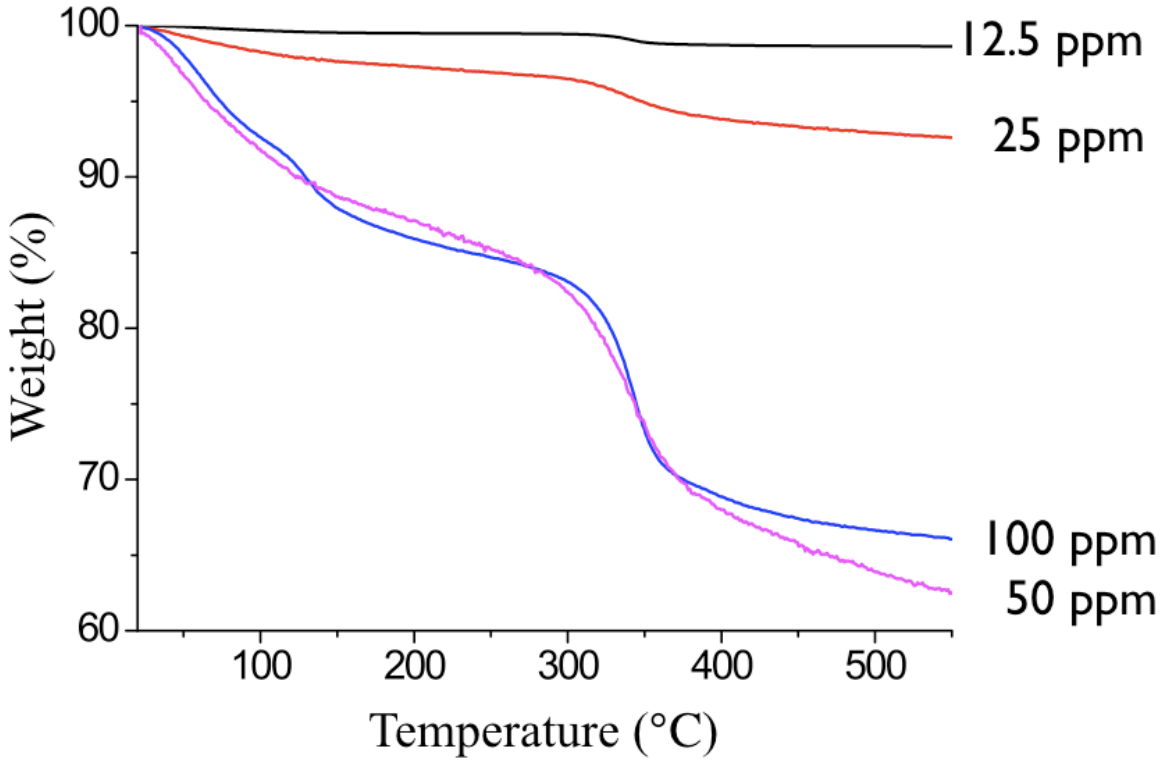

Figure S6. TGA profiles of $CaCO_3$ prepared with 12.5 ppm, 25 ppm, 50 ppm and 100 ppm SOM, respectively. The weight percentage of organics was determined from the loss of weight in the range 270°C to 415°C.

S7 Structure modifications in the shell of a diseased P. margaritifera.

(a)

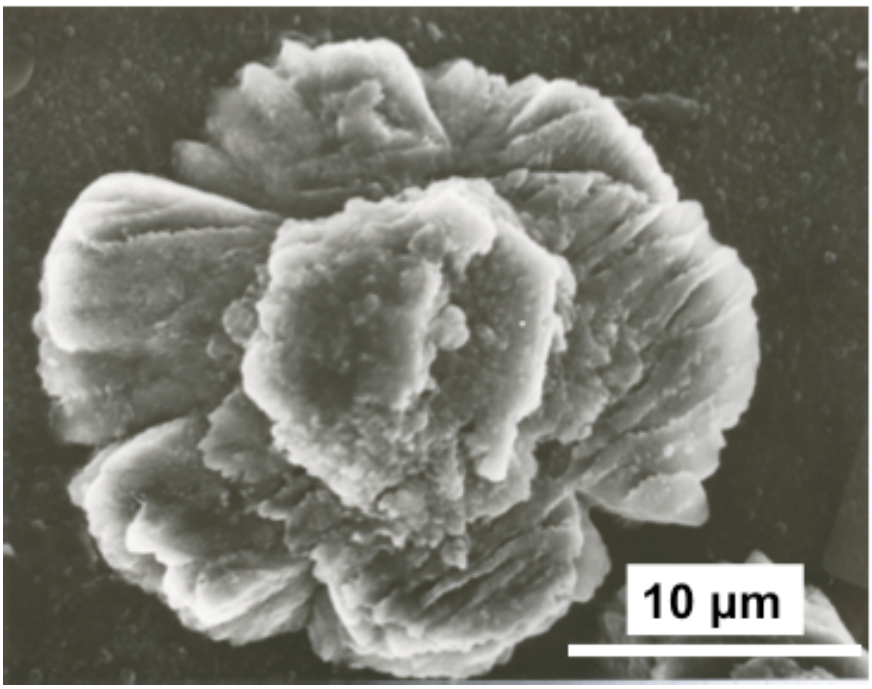

(b)

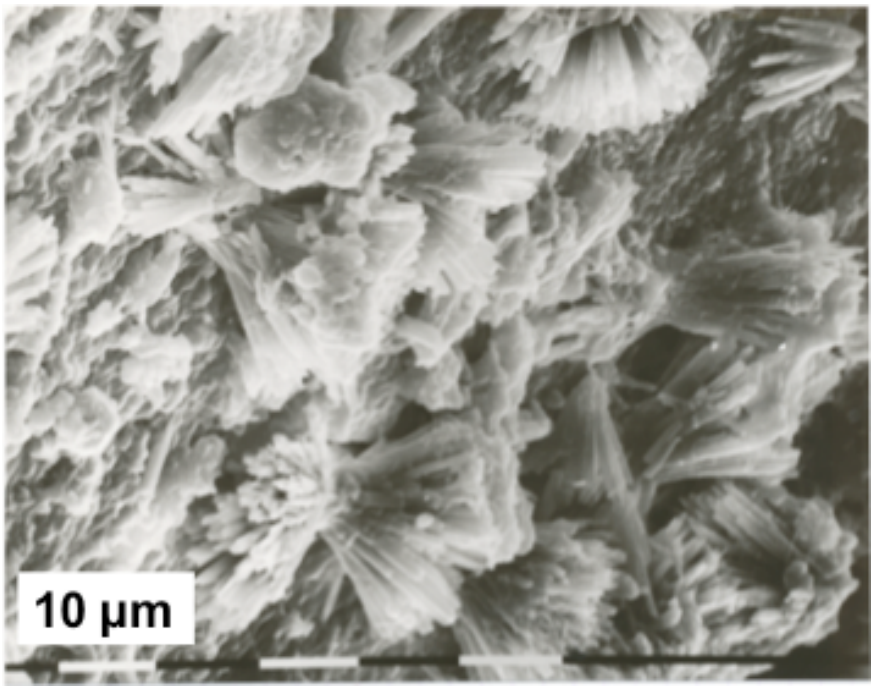

Figure S7. (a) SEM image of the inner surface of a valve of a diseased P. margaritifera. The hierarchical structure is preserved, but tablets are missing. (b) Inner surface of a valve of a diseased P. margaritifera showing spherulitic structure.